Journal of Magnetic Resonance **150,** 57–70 (2001)
doi:10.1006/jmre.2001.2312, available online at http://www.idealibrary.com on IDEAL®

Inverse Detection and Heteronuclear Editing in ^{1}H–^{15}N Correlation and ^{1}H–^{1}H Double-Quantum NMR Spectroscopy in the Solid State under Fast MAS

Ingo Schnell,* Benedikt Langer,* Serge H. M. Söntjens,† Marcel H. P. van Genderen,†
Rint P. Sijbesma,† and Hans Wolfgang Spiess*,[1]

*Max-Planck-Institut für Polymerforschung, Postfach 3148, D-55021 Mainz, Germany; and †Laboratory of Macromolecular and Organic Chemistry, Eindhoven University of Technology, P.O. Box 513, 5600 MB Eindhoven, The Netherlands

Received November 2, 2000; revised February 7, 2001; published online April 18, 2001

Signal enhancement in heteronuclear correlation spectra as well as signal selection in ^{1}H experiments can be achieved through inverse, i.e., ^{1}H, detection in the solid state under fast MAS conditions. Using recoupled polarization transfer (REPT), a heteronuclear ^{1}H–^{15}N single-quantum correlation (HSQC) experiment is presented whose symmetrical design allows the frequency dimensions to be easily interchanged. By observing the ^{15}N dimension indirectly and detecting on ^{1}H, the sensitivity is experimentally found to be increased by factors between 5 and 10 relative to conventional ^{15}N detection. In addition, the inverse ^{1}H–^{15}N REPT-HSQC scheme can be readily used as a filter for the ^{1}H signal. As an example, we present the combination of such a heteronuclear filter with a subsequent ^{1}H–^{1}H DQ experiment, yielding two-dimensional ^{15}N-edited ^{1}H–^{1}H DQ MAS spectra. In this way, specific selection or suppression of ^{1}H resonances is possible in solid-state MAS experiments, by use of which the resolution can be improved and information can be unravelled in ^{1}H spectra. © 2001 Academic Press

Key Words: **inverse detection; heteronuclear editing; double-quantum MAS spectroscopy; heteronuclear correlation spectroscopy; recoupled polarization transfer.**

1. INTRODUCTION

Solid-state NMR is increasingly being used for investigations of the structure and dynamics of complex materials, where particularly great demands on the sensitivity of the experiments as well as on the selectivity and specificity of the information obtainable from the spectra are made (*1, 2*). To achieve these goals, high magnetic fields of up to 17.6 T and higher as well as magic-angle sample spinning (MAS) at frequencies in excess of 30 kHz are applied. While the strength of the static magnetic field improves the sensitivity and the isotropic chemical-shift separation of the resonance lines, fast MAS enhances the spectral resolution by averaging anisotropic interactions. The combination of high fields and fast MAS has been shown to be of particular importance for ^{1}H NMR spectroscopy in the solid state (*3–8*), which is readily and routinely applicable to unmodified or as-synthesized samples due to the high natural abundance and the high magnetogyric ratio, γ_H, of ^{1}H nuclei. Although the wealth of information obtainable from ^{1}H solid-state MAS spectra should in general not be underestimated, there are certainly a number of cases where simple ^{1}H spectra do not fully meet the selectivity and specificity requirements because, for example, the signals of interest can be neither fully resolved nor distinguished from the ubiquitous and mostly intense ^{1}H background. In contrast, ^{13}C and ^{15}N nuclei, while lacking high natural abundance and requiring synthetically demanding isotopic enrichment procedures in most cases, have the advantage of a large chemical shift range and, hence, a much better resolution of chemically distinct sites is possible.

In order to combine the advantages of ^{1}H on the one hand with those of ^{13}C and ^{15}N on the other hand, various heteronuclear multidimensional correlation experiments have been introduced to solid-state NMR (*9–14*). These experiments basically consist of a frequency dimension for each nucleus of interest, linked by heteronuclear polarization transfer steps, including band-selective ones (*14*), with ^{1}H nuclei serving as an initial source of polarization. The analogy to established solution-state techniques is obvious, but instead of the J-coupling the heteronuclear dipolar interaction is commonly used for polarization transfer in the solid state (except for Ref. (*10*)). In addition to MAS, pulse sequences such as frequency-switched Lee–Goldburg (*15, 16*) can be applied during the ^{1}H dimension in order to improve the homonuclear dipolar decoupling and, in this way, narrow the ^{1}H resonance lines (*9, 10*). Alternatively, the experiments can be performed under very fast MAS, which, however, affects the heteronuclear dipolar couplings too, such that dipolar recoupling becomes an obvious way to ensure efficient polarization transfer (*11, 12*).

A versatile technique in the context of heteronuclear correlation experiments is inverse detection, which enhances the signal intensity by finally detecting on the high-γ nucleus ^{1}H, while the heteronuclei are observed indirectly. In solution-state NMR, inverse detection is well established and routinely applied

[1] To whom correspondence should be addressed. Fax: +49 6131 379 320. E-mail: spiess@mpip-mainz.mpg.de.

1090-7807/01 $35.00

(*17–23*). Although the idea was proposed at an early stage for solid-state applications (*24–29*), it has not yet attracted a comparable degree of attention and has only recently been reexamined by Ishii and Tycko (*30*) in the light of the latest technological developments, in particular fast MAS. However, in contrast to the dipolar recoupling technique presented below, the inverse ^{1}H–^{15}N experiment used in Ref. (*30*) is based on a sequential $^1\text{H} \rightarrow {}^{15}\text{N} \rightarrow {}^1\text{H}$ adiabatic cross polarization. The reluctance in solid-state NMR with respect to the adoption of inverse ^{1}H detection is predominantly due to the fact that in rigid systems ^{1}H resonances are only poorly resolved under moderate MAS conditions and then require the application of additional decoupling pulse sequences (*9, 10*). Another problem appears to arise from the assumed reliance of the inverse-detection techniques on pulsed-field gradients (PFGs) (*31–35*), which are not routinely available in solid-state NMR probes. However, as will also be demonstrated in the following, radiofrequency (RF) pulse schemes coupled with the performance of modern digital pulse-phase shifters allow a satisfactory suppression of unwanted ^{1}H signal in inversely detected spectra even without the help of PFGs.

The experimental methods introduced in this paper are based on heteronuclear correlation spectroscopy employing the recoupled polarization transfer (REPT) technique developed by Saalwächter *et al.* (*11–13*), which includes REDOR-type building blocks (*36*) and is also related to the TEDOR technique by Hing *et al.* (*37, 38*). In contrast to conventional cross polarization, REPT is a dedicated heteronuclear dipolar recoupling pulse sequence and, hence, allows efficient polarization transfer under fast MAS conditions, with the latter enhancing the ^{1}H spectral resolution. In addition, the design of the REPT approach, which inherently consists of *two* dipolar recoupling periods, readily enables the signal to be detected either conventionally on the heteronucleus or in the inverse fashion on ^{1}H. Since the inverse version effectively does not include a polarization transfer from ^{1}H to the heteronucleus, it bears some analogy to the dipolar heteronuclear single-quantum correlation (DIP-HSQC) experiment discussed in Ref. (*13*). Finally, inversely detected REPT correlations can also be used as a filter for subsequent ^{1}H experiments, such as ^{1}H–^{1}H double-quantum (DQ) experiments (*4, 39, 40*), which select ^{1}H resonances based on the presence of heteronuclear dipolar couplings and, in this way, enables heteronuclear editing of ^{1}H spectra.

2. METHODS

2.1. REPT-HSQC Spectra

The heteronuclear correlations explored here are based on dipole–dipole couplings between two types of spins, I and S. Under MAS conditions, the respective Hamiltonian reads

$$\mathbf{H}_\text{D}^{IS}(t) = -\omega_\text{D}^{IS}(t) \cdot 2\mathbf{I}_Z\mathbf{S}_Z. \qquad [1]$$

The time-dependent factor $\omega_\text{D}^{IS}(t)$ is the rotor-modulated spatial part of the dipolar interaction between the spins I and S,

$$\omega_\text{D}^{IS}(t) = D_{IS} \cdot \left[\frac{1}{2}\sin^2\beta_{IS}\cos(2\omega_\text{R}t + 2\gamma_{IS}) - \frac{1}{\sqrt{2}}\sin 2\beta_{IS}\cos(\omega_\text{R}t + \gamma_{IS})\right], \qquad [2]$$

where ω_R is the MAS frequency, and β_{IS} and γ_{IS} denote the azimuthal and polar angle, respectively, of the vector r_{IS} connecting the two nuclei. D_{IS} is the dipolar coupling constant (in units of angular frequency),

$$D_{IS} = \frac{\mu_0}{4\pi} \cdot \frac{\gamma_I\gamma_S\hbar}{r_{IS}^3}, \qquad [3]$$

where γ_I and γ_S denote the magnetogyric ratios of the I and S spins, and r_{IS} is the distance between the two coupled nuclei. To account for the averaging effect of MAS, in general the average Hamiltonian

$$\bar{\mathbf{H}}_\text{D}^{IS}(t_1, t_2) = \frac{1}{t_2 - t_1}\int_{t_1}^{t_2}\mathbf{H}_\text{D}^{IS}(t)\,dt \qquad [4]$$

must be considered (*1*). Note that the integral of the heteronuclear dipolar interaction, Eqs. [1] and [2], vanishes for a full rotor period, $t_2 - t_1 = \tau_\text{R}$. For polarization transfer between I and S, the dipolar interaction can be recoupled by inverting the sign of the spin part, $\mathbf{I}_Z\mathbf{S}_Z$, every other half rotor period. This can be easily accomplished by the application of π-pulses at intervals of $\tau_\text{R}/2$ on either the I or the S spins (*36, 41*). In addition, the π-pulses refocus chemical shift and resonance offset effects. The recoupled average Hamiltonian is then given by

$$\bar{\mathbf{H}}_\text{D}^{IS}(0, N\tau_\text{R}) = -\Omega_\text{D}^{IS}(0, N\tau_\text{R}) \cdot \mathbf{I}_Z\mathbf{S}_Z \qquad [5]$$

with the integrated spatial part

$$\Omega_\text{D}^{IS}(0, N\tau_\text{R}) = N \cdot \frac{D_{IS}}{\omega_\text{R}} 2\sqrt{2}\sin 2\beta_{IS}\sin\gamma_{IS}, \qquad [6]$$

where N denotes the number of rotor cycles, during which the train of π-pulses recouples the dipolar interaction. In a REPT-HSQC experiment, whose pulse sequence is depicted in Fig. 1a, the dipolar recoupling periods are responsible for the polarization transfer from I to S. (The experiment is described in detail in Refs. (*12*) and (*13*), and for the reader's convenience its main features are summarized here.) After the initial $\pi/2$-pulse on I (with phase x), the transverse magnetization, $-\mathbf{I}_Y$, is subject to $\bar{\mathbf{H}}_\text{D}^{IS}$ for a period $N\tau_\text{R}$, resulting in a state

$$-\mathbf{I}_Y \xrightarrow{\bar{\mathbf{H}}_\text{D}^{IS}(0, N\tau_\text{R})} -\mathbf{I}_Y \cdot \cos\Omega_\text{D}^{IS}(0, N\tau_\text{R}) + \mathbf{I}_X\mathbf{S}_Z \cdot \sin\Omega_\text{D}^{IS}(0, N\tau_\text{R}). \qquad [7]$$

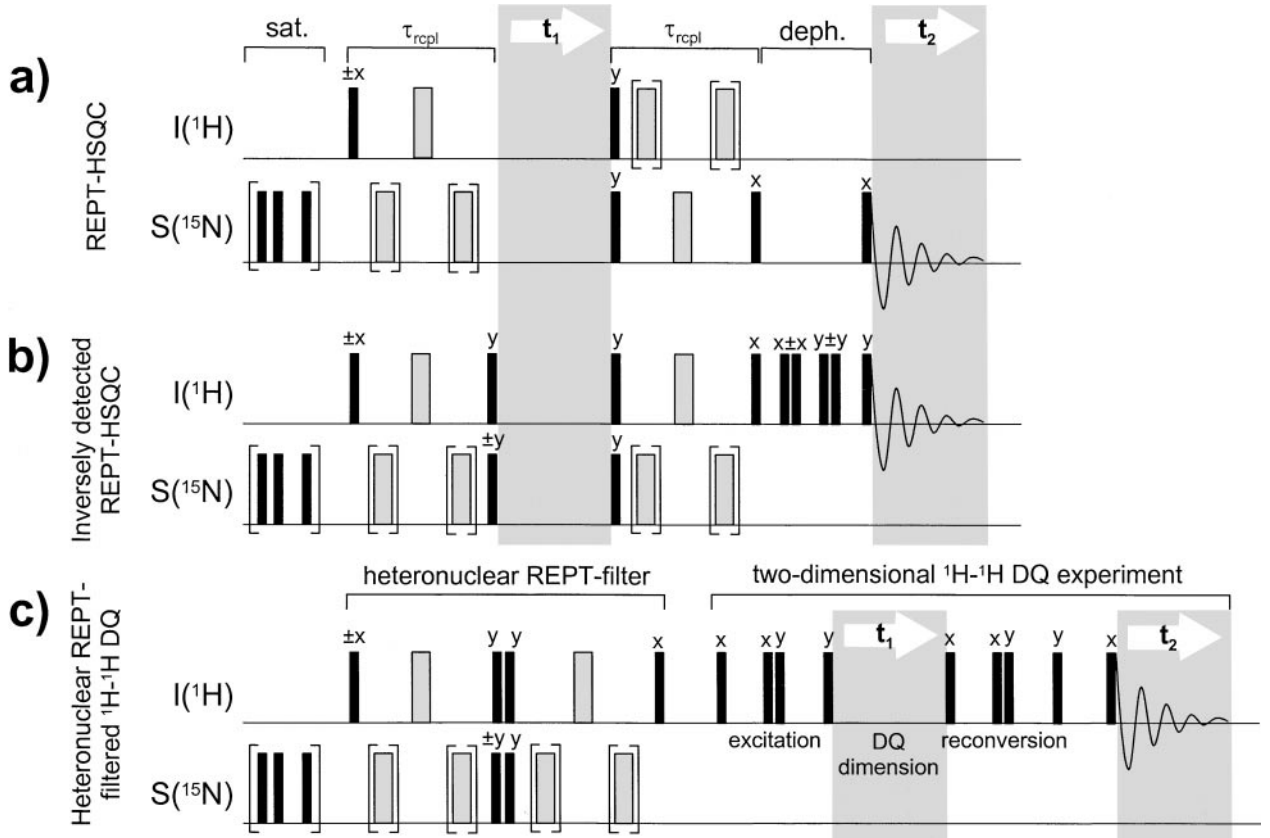

FIG. 1. Schematic representations of the pulse sequences used for the two-dimensional MAS NMR experiments presented here: (a) REPT-HSQC experiment, (b) inversely detected REPT-HSQC, (c) heteronuclear REPT-HSQC filtered ^{1}H–^{1}H DQ experiment. Radiofrequency $\pi/2$- and π-pulses are denoted by black and gray boxes, respectively. The π-pulses in the recoupling periods are separated by half rotor periods, and the bracketed ones are applied either once or three times to achieve heteronuclear dipolar recoupling for durations, τ_{rcpl}, of either two or four rotor periods, respectively. The initial train of $\pi/2$-pulses on S is applied for saturation purposes.

The residual transverse I-magnetization is removed by phase cycling from the signal and is therefore neglected. The mixed state, $\mathbf{I}_X\mathbf{S}_Z$, experiences I chemical-shift evolution during t_1 according to $\mathbf{H}^I_{\mathrm{CS}} = \omega^I_{\mathrm{CS}} \cdot \mathbf{I}_Z$, in the course of which a superposition of $\mathbf{I}_X\mathbf{S}_Z$ and $\mathbf{I}_Y\mathbf{S}_Z$ is created:

$$\begin{aligned}&\mathbf{I}_X\mathbf{S}_Z \cdot \sin\Omega^{IS}_{\mathrm{D}}(0, N\tau_{\mathrm{R}})\\ &\xrightarrow{\omega^I_{\mathrm{CS}}\mathbf{I}_Z} \left(\mathbf{I}_X\mathbf{S}_Z \cdot \cos\left(\omega^I_{\mathrm{CS}}t_1\right) + \mathbf{I}_Y\mathbf{S}_Z \cdot \sin\left(\omega^I_{\mathrm{CS}}t_1\right)\right)\\ &\qquad \cdot \sin\Omega^{IS}_{\mathrm{D}}(0, N\tau_{\mathrm{R}}).\end{aligned} \quad [8]$$

A $\pi/2$-pulse of phase x or y and a $\pi/2$-pulse of phase y are then applied to I and S, respectively, converting the state to a superposition of $\mathbf{I}_\alpha\mathbf{S}_X$ with $\alpha = x, y, z$. Only the longitudinal I-component, i.e., the state $\mathbf{I}_Z\mathbf{S}_X$, will finally contribute to the signal, such that the phase of the $\pi/2$-pulse applied to I after t_1 can be used to ensure phase-sensitive detection in t_1, for example by means of TPPI (*42*). During the second period of heteronuclear dipolar recoupling, the mixed state $\mathbf{I}_Z\mathbf{S}_X$ is converted to transverse S-magnetization, $\mathbf{S}_X$, which is detected after passing through a z-filter. This filter reduces residual transverse magnetization by dephasing and, more importantly, enables symmetrical coherence transfer pathways and, hence, ensures pure amplitude modulation of the signal. Thus, the signal components, S_X and S_Y, of the HSQC spectrum are given by (*12*)

$$S_X(\mathbf{S}) \propto \left\langle \cos\left(\omega^I_{\mathrm{CS}}t_1\right) \cdot \sin\Omega^{IS}_{\mathrm{D}}(0, N\tau_{\mathrm{R}}) \cdot \sin\Omega^{IS}_{\mathrm{D}}(t_1, t_1 + N\tau_{\mathrm{R}})\right\rangle \quad [9a]$$

and

$$S_Y(\mathbf{S}) \propto \left\langle \sin\left(\omega^I_{\mathrm{CS}}t_1\right) \cdot \sin\Omega^{IS}_{\mathrm{D}}(0, N\tau_{\mathrm{R}}) \cdot \sin\Omega^{IS}_{\mathrm{D}}(t_1, t_1 + N\tau_{\mathrm{R}})\right\rangle. \quad [9b]$$

The brackets $\langle\cdots\rangle$ indicate the orientational averaging procedure which must be carried out for powdered samples.

In the correlation experiments discussed here, the t_1 dimension is incremented in a "rotor-synchronized" fashion, i.e., in intervals of full rotor periods. In this way, the generation of MAS sidebands in the indirect dimension as a consequence of a

t_1 phase shift between the two dipolar recoupling periods is prevented. The use of finer t_1-increments leads to MAS sidebands due to the rotor encoding of the recoupled Hamiltonian (*4, 39, 43,*) which can serve as a precise measure for the strength of the underlying couplings (*8, 11, 12, 44, 45*). In rotor-synchronized spectra, the signal simplifies to

$$S_X(\mathbf{S}) \propto \left\langle \cos\left(\omega_{\mathrm{CS}}^I t_1\right) \cdot \sin^2 \Omega_{\mathrm{D}}^{IS}(0, N\tau_{\mathrm{R}}) \right\rangle \qquad [10a]$$

and

$$S_Y(\mathbf{S}) \propto \left\langle \sin\left(\omega_{\mathrm{CS}}^I t_1\right) \cdot \sin^2 \Omega_{\mathrm{D}}^{IS}(0, N\tau_{\mathrm{R}}) \right\rangle, \qquad [10b]$$

such that the chemical shifts of I and S are correlated, and the signal intensity is weighted by the IS heteronuclear dipolar coupling.

2.2. Inversely Detected REPT-HSQC Spectra

Due to its design, the regular REPT-HSQC experiment described above can in principle be easily changed to an inverse type of experiment, where the S-spins are indirectly observed during t_1, while the I-spins are detected during t_2. The first modification is the insertion of two $\pi/2$-pulses applied to I and S at the start of the t_1 dimension. After the first recoupling period, these pulses interchange the transverse and longitudinal components in the mixed state from $\mathbf{I}_X\mathbf{S}_Z$ (see Eq. [7]) to $\mathbf{I}_Z\mathbf{S}_X$, such that the chemical-shift evolution occurs on the S-spins during t_1:

$$\begin{aligned} &\mathbf{I}_Z\mathbf{S}_X \cdot \sin \Omega_{\mathrm{D}}^{IS}(0, N\tau_{\mathrm{R}}) \\ &\xrightarrow{\omega_{\mathrm{CS}}^S S_Z} \left(\mathbf{I}_Z\mathbf{S}_X \cdot \cos\left(\omega_{\mathrm{CS}}^S t_1\right) + \mathbf{I}_Z\mathbf{S}_Y \cdot \sin\left(\omega_{\mathrm{CS}}^S t_1\right)\right) \\ &\qquad \cdot \sin \Omega_{\mathrm{D}}^{IS}(0, N\tau_{\mathrm{R}}). \end{aligned} \qquad [11]$$

After t_1, the inverse experiment proceeds identically to the regular one except that I and S are interchanged, i.e., the z-filter as well as the final detection takes place on the I-spins. Thus, in a rotor-synchronized inversely detected HSQC spectrum, the signal also consists of the following components:

$$S_X(\mathbf{I}) \propto \left\langle \cos\left(\omega_{\mathrm{CS}}^S t_1\right) \cdot \sin^2 \Omega_{\mathrm{D}}^{IS}(0, N\tau_{\mathrm{R}}) \right\rangle \qquad [12a]$$

and

$$S_Y(\mathbf{I}) \propto \left\langle \sin\left(\omega_{\mathrm{CS}}^S t_1\right) \cdot \sin^2 \Omega_{\mathrm{D}}^{IS}(0, N\tau_{\mathrm{R}}) \right\rangle. \qquad [12b]$$

Comparing Eqs. [10a, 10b] and [12a, 12b], it is clear that inverse and regular detection lead to the same two-dimensional correlation spectrum except for an interchange of the frequency axes. From an experimental point of view, however, there is more than a simple change of axes, because usually the two types of nuclei differ considerably in their magnetogyric ratios and their abundance. In practice, the I-spins are commonly ^{1}H, while the S-spins are, for example, ^{13}C or ^{15}N either in natural abundance or, more frequently, in isotopic enrichment. Hence, the magnetogyric ratio, γ_I, of the I-spins is higher by a factor of 4 or even 10, which in principle leads to an increase in sensitivity by a factor $(\gamma_I/\gamma_S)^{3/2}$ for the signal detection. Before turning to the discussion of the sensitivity enhancement which can be expected to be gained by inverse detection in practice, we shall briefly address the experimental complications which arise from a marked difference in abundance between I- and S-spins.

Usually, the basic experimental problem of inverse detection is that a large amount of I-spin signal does not stem from IS-correlations, but from uncoupled I-spins, and therefore needs to be subtracted or, better still, to be suppressed during the detection. An elegant and well established way to suppress such unwanted I-spin signal efficiently is the application of PFGs for selective dephasing and rephasing of polarization, which is routinely used in solution or liquid-state NMR (*31–35*). Such PFGs, however, are often not available in solid-state NMR probes (as examples for solid-state PFGs, see Refs. (*46–48*)) and, moreover, difficulties would arise from the fact that the transverse relaxation times are usually considerably shorter in solids, in particular for ^{1}H, than in solutions or liquids, thereby limiting the time window for PFGs in solid-state experiments.

Without PFGs, the signal selection relies on phase cycles causing sign inversions of the IS-correlations such that the unwanted I-spin signal is subtracted in every other transient. Although the receiver must then be adjusted to the intense overall I-spin signal and cannot accomodate the relatively weak signal which has passed through IS-correlations, the precision of modern digital phase shifters and receivers allows a satisfactory signal subtraction. Additional purification of the signal can be achieved by introducing four $\pi/2$-pulses into the z-filter before the final detection period (see Fig. 1b). One of the purposes of the z-filter is the suppression of residual transverse ^{1}H polarization by dephasing. However, the duration of the filter and, hence, its dephasing efficiency is limited by the time scale on which ^{1}H–^{1}H spin diffusion sets in. The four pulses help with the suppression in that they are applied with phases (x, x, y, y) and $(x, -x, y, -y)$ in subsequent transients, while the receiver phase remains unchanged. In this way, longitudinal magnetization is unaffected, whereas components of transverse polarization experience a sign inversion every other transient such that their signal contributions cancel.

Certainly the major goal targeted on by inverse detection schemes is sensitivity enhancement, which has recently been addressed in detail by Ishii and Tycko for the case of ^{1}H–^{15}N in the solid state (*30*). Apart from the obvious advantage of the high ^{1}H magnetogyric ratio, the dependence of the resulting experimental sensitivity is rather complex and involves also the Q-factors of the probe at the I- and S-resonance frequencies as well as the experimental I-spin, i.e., ^{1}H, linewidth. While the ^{1}H linewidth can be significantly narrowed by fast MAS, as has already been demonstrated extensively (*3–6, 8*), the Q-factors depend on the individual designs and performances of the probes, which are, for standard solid-state applications,

usually not optimized for ^{1}H detection. Furthermore, with respect to two-dimensional correlation spectra, the comparison between regular and inverse detection must take into account the number of data points to be recorded for the I- and S-spin FIDs, and the effect on the experiment time, when the direct and indirect dimensions are interchanged. In comparison to ^{13}C or ^{15}N, the overall width of ^{1}H spectra is less and, even under fast MAS, ^{1}H lines are invariably broader in the solid state. Consequently, the number of data points required for ^{1}H FIDs is usually significantly smaller than for ^{13}C or ^{15}N FIDs. In this respect, the ^{1}H signal should preferably be observed during the t_1 dimension, because the experiment time increases linearly with the number of data points recorded in the indirect (t_1) dimension, while the number of data points recorded in the direct (t_2) dimension has practically no effect. Hence, if the FID of the heteronucleus requires n times more data points than the ^{1}H FID, and the total experiment time shall be kept constant, the number of scans must be reduced to $1/n$ for inverse, i.e.,^{1}H, detection compared to regular detection of the heteronucleus.

2.3. REPT-HSQC Edited ^{1}H–^{1}H DQ Spectra

As well as being used for ^{1}H detection, inversely detected heteronuclear correlation experiments can also serve as a building block in ^{1}H experiments, which allows the selection of specific ^{1}H resonances for subsequent homonuclear ^{1}H NMR methods. By omitting the t_1 evolution period, i.e., $t_1 = 0$, the inversely detected REPT-HSQC experiment is effectively changed to a filter for the signals of I-spins which are involved in a dipolar IS-correlation. According to Eqs. [12a, 12b], such a REPT-HSQC filter leads to an effective I-spin magnetization of

$$M(\mathbf{I}) \propto \left\langle \sin^2 \Omega_{\mathrm{D}}^{IS}(0, N\tau_{\mathrm{R}}) \right\rangle \approx \left\langle \left(\Omega_{\mathrm{D}}^{IS}(0, N\tau_{\mathrm{R}})\right)^2 \right\rangle \quad \text{for } \Omega_{\mathrm{D}}^{IS}(0, N\tau_{\mathrm{R}}) < 1, \quad [13]$$

which can then serve as the initial state for a subsequent experiment on the I-spins. The approximation is valid in the limit of short recoupling times and/or weak dipolar couplings (*4, 6*), and it shows that the filtered magnetization is weighted by the heteronuclear coupling constant according to D_{IS}^2 and, hence, by the internuclear distance according to r_{IS}^{-6}. In addition, an orientational weighting factor of $\sin 2\beta_{IS} \sin \gamma_{IS}$ is introduced (see Eq. [6]). While the latter can only be exploited for samples with uniformly oriented molecules, the former results in an efficient selection of I-spins which exhibit a close proximity to S-spins, i.e., in particular for chemically bonded IS-pairs.

Such a REPT-HSQC filter can, for example, be coupled with a two-dimensional ^{1}H–^{1}H DQ MAS experiment. The versatility of the latter has recently been demonstrated for a variety of applications (*3, 5, 8, 49, 50*). The basic principle underlying homonuclear dipolar DQ MAS approaches is the exploitation of homonuclear dipole–dipole couplings for the generation of double-quantum coherences (DQCs). Conversely the observation of such coherences implies the existence of a sufficient dipole–dipole coupling between the respective nuclei. In the case of a dipolar-coupled II'-spin pair, the DQ signal intensity, which is excited and reconverted during dipolar recoupling periods of duration $M\tau_{\mathrm{R}}$, is given by

$$S_{\mathrm{DQ}}(\mathbf{I}) \propto \left\langle \sin^2 \Omega_{\mathrm{D}}^{II'}(0, M\tau_{\mathrm{R}}) \right\rangle \approx \left\langle \left(\Omega_{\mathrm{D}}^{II'}(0, M\tau_{\mathrm{R}})\right)^2 \right\rangle \quad \text{for } \Omega_{\mathrm{D}}^{II'}(0, M\tau_{\mathrm{R}}) < 1, \quad [14]$$

where the approximation is again valid for short recoupling times and/or weak dipolar couplings. The integrated spatial part of the homonuclear dipole–dipole coupling reads

$$\Omega_{\mathrm{D}}^{II'}(0, M\tau_{\mathrm{R}}) = -N \cdot \frac{D_{II'}}{\omega_{\mathrm{R}}} \cdot \frac{3}{2}\sqrt{2} \sin 2\beta_{II'} \sin \gamma_{II'}. \quad [15]$$

Note the analogy between homonuclear DQ and heteronuclear correlation signal intensities in Eqs. [14] and [12a, 12b], which is due to the fact that both signals arise from recoupled dipolar interactions (see Eqs. [15] and [6], respectively).

Two-dimensional DQ spectra (*4, 39, 40*) correlate a DQ spectral dimension (t_1) with a SQ dimension, with the latter being used for signal detection. In the DQ dimension, each observed resonance frequency, ω_{AB}, corresponds to the sum frequency of the two nuclei, A and B, involved in the coherence: $\omega_{\mathrm{AB}} = \omega_{\mathrm{A}} + \omega_{\mathrm{B}}$. In this way, the signal pattern of ^{1}H–^{1}H DQ spectra provides detailed information about proximities between spectrally resolved protons. In this context, even under fast MAS, a reduction or, preferably, a specific selection of DQ signals would be useful in some cases. The pulse sequence for a REPT-HSQC filtered two-dimensional ^{1}H–^{1}H DQ experiment is depicted in Fig. 1c (the four pulses applied during the z-filter in Fig. 1b can be omitted, because the following DQ pulse sequence ensures sufficient suppression of unwanted transverse ^{1}H magnetization). In the filtered version, the DQ experiment effectively starts with the magnetization of only those protons which are strongly dipolar-coupled to the respective heteronucleus. During t_2, the signal is then detected on protons which are involved in a DQC with the previously selected ones. In a first approximation, the intensity of a REPT-HSQC filtered homonuclear DQ signal is given by the combination of Eqs. [13] and [14]:

$$S_{\mathrm{DQ,filt}}(\mathbf{I}, \mathbf{I}') \propto \left\langle \left\lfloor \left(\Omega_{\mathrm{D}}^{IS}(0, N\tau_{\mathrm{R}})\right)^2 + \left(\Omega_{\mathrm{D}}^{I'S'}(0, N\tau_{\mathrm{R}})\right)^2 \right\rfloor \cdot \left(\Omega_{\mathrm{D}}^{II'}(0, M\tau_{\mathrm{R}})\right)^2 \right\rangle. \quad [16]$$

Note that the DQC can involve either two protons or only one selected through REPT-HSQC. In both cases, DQ signals are observed, but in the latter situation the initial magnetization stems from only one of the two protons, such that the signal intensity is usually significantly reduced.

3. SAMPLES AND EXPERIMENTS

To demonstrate the feasibility of inverse detection and heteronuclear editing for ^{1}H–^{15}N HSQC and ^{1}H–^{1}H DQ experiments in the solid state, samples of *N*-butylaminocarbonyl-6-tridecyl isocytosine were chosen. The molecules are capable of dimerizing through the formation of a directed quadruple hydrogen bond and have been successfully used as linking units for supramolecular polymers (*53, 54*). Therefore, the molecular unit has recently attracted considerable interest in the field of supramolecular chemistry, where noncovalent interactions are increasingly being used to enable the assembling of well-defined structures, following the concept of self-assembly of synthetic molecules by the molecular recognition of complementary components (*51*). In biology, the same principle of structure determination through noncovalent interactions is, for example, reflected in the hydrogen-bonded base pairs of DNA.

In addition, *N*-butylaminocarbonyl-6-tridecyl isocytosine can adopt two tautomeric structures, 4[^{1}H]-pyrimidinone (keto) and pyrimidin-4-ol (enol), both of which dimerize through a quadruple hydrogen bond (see Fig. 2)(*52–55*). The synthesis was started using $^{15}N_1$-guanidine, C(*NH)$(NH_2)_2$, such that in the resulting molecules one of the three nitrogens belonging to the isocytosine unit is ^{15}N, and the isotopic enrichment is equally distributed over the three positions in the sample. The keto and enol form of the dimers was obtained by recrystallizing the material from $CHCl_3$ and DMF, respectively. From the NMR point of view, the tridecyl substituents ($C_{13}H_{27}$) give rise to intense methylene ^{1}H signals, which are to be suppressed by the ^{1}H–^{15}N REPT-HSQC filter, thereby allowing the demonstration of its experimental selection efficiency. Moreover, N···H···N and N···H···O hydrogen bonds have been shown to be well suited to ^{1}H solid-state investigations employing fast MAS and ^{1}H–^{1}H DQ methods (*5*).

The NMR experiments were performed using a Bruker DRX spectrometer with a 2.5-mm double-resonance MAS probe, operating at ^{1}H and ^{15}N Larmor frequencies of 700.1 and 70.9 MHz, respectively. The ^{15}N CPMAS spectra were recorded under MAS at 3.2 kHz, while for all other experiments fast MAS at 30 kHz was used. The RF pulses were applied at a B_1-field strength of 83.3 kHz, corresponding to a pulse width of 3 μs for $\pi/2$-pulses, while the ^{1}H–^{15}N cross polarization was performed using weaker RF fields of approximately 70 kHz with a ramp on ^{15}N, followed by ^{1}H TPPM-decoupling (*56*) at 62.5 kHz. Under fast MAS, ^{15}N detection was also carried out under ^{1}H TPPM-decoupling at 62.5 kHz, while ^{1}H detection was not found to be improved by ^{15}N CW- or TPPM-decoupling, which was therefore omitted. The indirect dimensions, t_1, of the two-dimensional experiments were incremented in steps of full rotor periods, such that the generation of MAS sidebands is avoided in this frequency dimension. The recycle times were 2 and 5 s for the keto and the enol compounds, respectively.

In the REPT periods of the experiments, the heteronuclear ^{1}H–^{15}N dipolar interaction is recoupled for a duration of either two or four rotor periods, i.e., 66.6 or 133.3 μs, respectively, which corresponds to the application of each of the bracketed π-pulses in Figs. 1a and 1b either once or three times. For filtration purposes (Fig. 1c), only short recoupling periods of 66.6 μs are used. In the ^{1}H–^{1}H DQ experiments, the homonuclear ^{1}H–^{1}H dipolar interaction is recoupled using the BaBa pulse sequence (*4, 57*) for one rotor period, i.e., 33.3 μs. In the ^{15}N-detecting REPT-HSQC experiments (schematically shown Fig. 1a), the signal is selected through a phase alternation ($\pm$) of the first ^{1}H $\pi/2$-pulse, followed by a corresponding phase alternation of the receiver. To achieve phase-sensitive detection of the indirect dimension by means of a TPPI procedure (*42*), the phase of the second ^{1}H $\pi/2$-pulse is incremented in steps of 90° simultaneously to the incrementation of t_1.

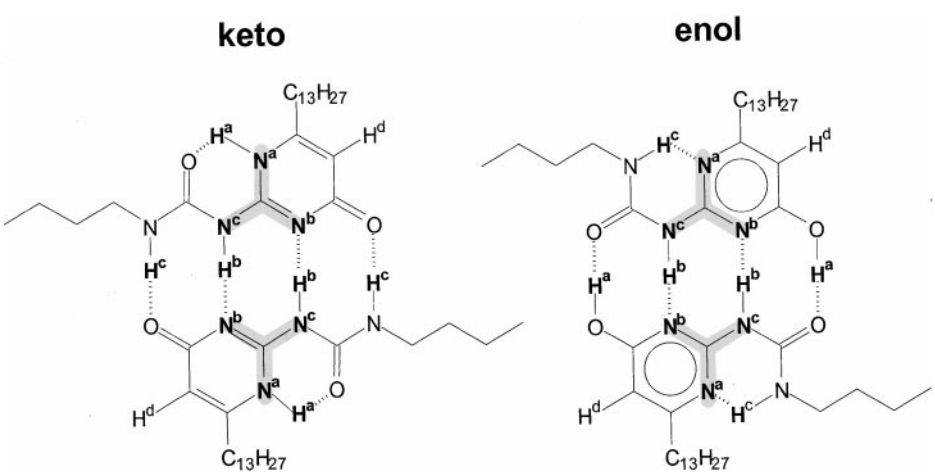

FIG. 2. Molecular structures of the samples investigated here: two tautomeric types of quadruply hydrogen-bonded dimers of *N*-butylaminocarbonyl-6-tridecyl isocytosine. In each molecule, one of the nitrogens in the isocytosine unit (shaded) is ^{15}N-labeled, such that over the whole sample, the three different positions are ^{15}N-enriched to the same extent.

In the ^{1}H-detecting REPT-HSQC experiments (schematically shown in Fig. 1b), the signal is selected through a nested phase alternation of the first ^{1}H and ^{15}N $\pi/2$-pulses. In addition, the suppression of residual transverse polarisation during the z-filter is supported by four $\pi/2$-pulses, the effect of which has already been described in Section 2.2. In the REPT-filtered ^{1}H–^{1}H DQ experiments, these four pulses can be omitted (see above), and the ^{1}H/^{15}N phase alternations are combined with two nested four-step phase cycles which select the ^{1}H coherence transfer pathway $0 \rightarrow \pm 2 \rightarrow 0 \rightarrow -1$ during the DQ experiment.

In order to compare the experimental performance of the ^{15}N- and ^{1}H-detected REPT-HSQC versions, the overall number of signal accumulations, i.e., the experiment time, was kept constant, while the number of data points recorded during t_1 and t_2 was adjusted according to the lengths of the ^{15}N and ^{1}H FIDs. For the ^{15}N-detected REPT-HSQC spectra, the t_1 (^{1}H) dimension consisted of 32 increments with 432 transients being accumulated. In the ^{1}H-detected version, the t_1 (^{15}N) dimension was extended to 108 increments, while averaging over only 128 transients. Hence, the total experiment time was about 7.5 and 19 h for the keto and enol compounds, respectively.

4. RESULTS AND DISCUSSION

4.1. ^{1}H MAS and ^{15}N CPMAS Spectra

In order to provide a first characterization of the two tautomeric compounds investigated in the following, ^{1}H MAS and ^{15}N CPMAS spectra are displayed in Fig. 3. In the ^{1}H one-pulse spectra recorded under MAS at 30 kHz, five resonances are clearly resolved (Figs. 3a and 3b): the three protons involved in hydrogen bonds (denoted H^a, H^b, and H^c), the vinyl or aromatic proton (H^d), and the aliphatic protons (H^{aliph}). The assignment of the protons H^a, H^b, and H^c (see molecular structures in Fig. 2) is aided by previous solution-state NMR investigations (*54*) and will be confirmed by the ^{1}H–^{1}H DQ spectra discussed in Section 4.3. The ^{15}N CPMAS spectra (Figs. 3c and 3d) show three resonances, corresponding to the three nitrogen positions of the isocytosine unit with ^{15}N isotope enrichment. The chemical shift positions (*58*) as well as the width of the MAS sideband patterns permit a clear distinction between the two types of ^{15}N nuclei. The resonance lines around -250 ppm with a narrow sideband pattern are characteristic for secondary amides of the form NHRR′, while the (isotropic) resonances around –170 ppm with a broad sideband pattern, indicating a large chemical shift anisotropy, are typical for tertiary amides where the nitrogen atom is part of a C=N double bond.

Comparing the spectra of the keto (Figs. 3a and 3c) and the enol forms (Figs. 3b and 3d), obvious differences are observed. In the ^{1}H spectra, the resonance positions of the protons forming hydrogen bonds are more separated for the enol tautomer. Upon going from the keto to the enol form, the ^{1}H chemical shifts changes are 13.2 $\rightarrow$ 13.6 ppm (H^a), 11.8 $\rightarrow$ 11.0 ppm (H^b), and 10.3 $\rightarrow$ 9.0 ppm (H^c), which can be attributed to modifications in the hydrogen bonds associated with the structural differences between the two tautomeric forms of the dimers. Furthermore, the aliphatic resonance line of the enol is significantly

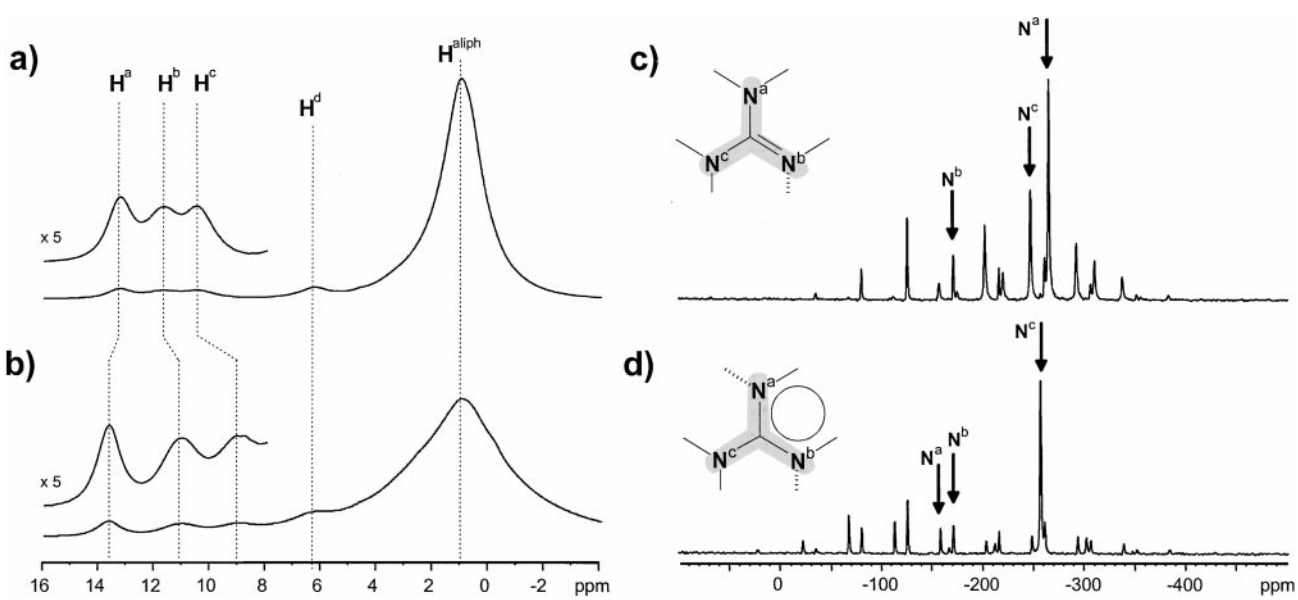

FIG. 3. ^{1}H one-pulse MAS (a and b, spinning at 30 kHz) and ^{15}N CPMAS (c and d, spinning at 3.2 kHz) spectra of the keto (a, c) and enol (b, d) forms of the hydrogen-bonded dimers shown in Fig. 2. In the ^{1}H spectra, the three protons involved in hydrogen bonds (H^a, H^b, and H^c), the vinyl or aromatic proton (H^d), and the aliphatic protons (H^{aliph}) are resolved. The ^{15}N CPMAS spectra show three resonances, corresponding to the three nitrogen positions of the isocytosine unit with ^{15}N isotope enrichment. The assignment of the resonances is discussed in the text.

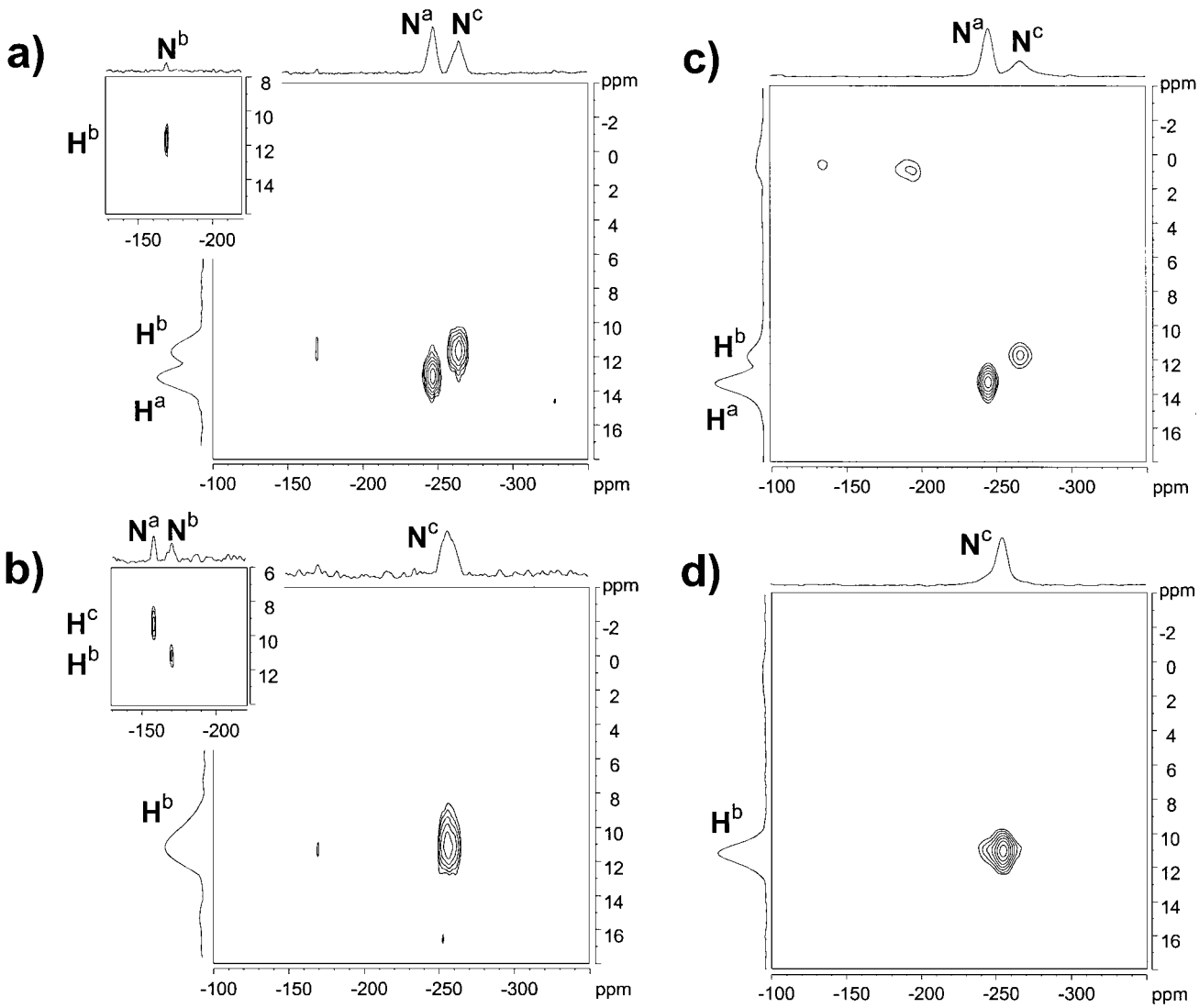

FIG. 4. ^{1}H–^{15}N REPT-HSQC spectra of the keto (a and c) and the enol (b and d) compounds, recorded under MAS at 30 kHz using heteronuclear dipolar recoupling periods of 66.6 μs (=2 τ_R). The experiments are performed with ^{15}N-detection (a and b) and, inversely, with ^{1}H-detection (c and d). The insets show regions of correlation spectra obtained for recoupling periods of 133.3 μs (=4 τ_R).

broader than for the keto form, indicating stronger dipolar interactions among the aliphatic protons and, hence, less mobility and a closer packing of the alkyl chains in the enol compound. The ^{15}N spectra clearly reflect the presence of two secondary-amide resonances for the keto form, while for the enol form only one secondary amide is present, but here two ^{15}N are involved in C=N double bonds. These features agree with the structure of the isocytosine unit in the two tautomers and allow the assignment of the N^b and N^c resonances for the keto and enol form, respectively. In order to unambiguously assign N^a and N^c in the keto spectrum (Fig. 3c) as well as N^a and N^b in the enol spectrum (Fig. 3d), additional information is required, which can be obtained from ^{1}H–^{15}N correlation spectra in combination with ^{1}H–^{1}H DQ spectra, as shown below.

4.2. ^{1}H–^{15}N REPT-HSQC Spectra with and without Inverse Detection

Since the intensities of ^{1}H–^{15}N REPT-HSQC signals exhibit a r_{NH}^{-6}-dependence on the NH distance, r_{NH}, the correlations of chemically bonded NH pairs are expected to be by far the strongest peaks in the spectra recorded for short recoupling times. Consider first the spectra obtained with regular ^{15}N-detection for the two tautomeric structures (Figs. 4a and 4b). For the keto form, two strong correlations H^a-N^a and H^b-N^c are observed, while for the enol form, the spectrum shows only one strong H^b-N^c correlation. In both cases, the number of strong correlations corresponds to the chemically bonded NH pairs of the isocytosine units, namely two in the keto and one in the enol form (see Fig. 2), which indicates that the chemical NH bonds

present in the single molecules still exist despite of the formation of hydrogen-bonded dimers. Thus, based on the ^{1}H assignment, which is known from ^{1}H–^{1}H DQ spectra (see section 4.3), an unambiguous assignment of the ^{15}N resonances is possible. In addition to the intense peaks, there is evidence for weak NH correlations in the spectra, which reflect the second shortest NH distances in the material, i.e. the N···H hydrogen bonds. For longer recoupling times, these weak signals become clearer in the spectra (as shown in the insets of Figs. 4a and 4b) and can directly be assigned to the hydrogen bonds in the keto and enol dimers, respectively (see Fig. 2).

The inversely detected REPT-HSQC spectra (Figs. 4c and 4d) are basically identical to the ^{15}N-detected ones discussed above, exhibiting the same characteristic NH correlations. Only a few minor differences to the spectra obtained with ^{15}N-detection can be noticed, such as the presence of traces of signal at the aliphatic ^{1}H resonance (see Fig. 4c) as well as slightly reduced ^{1}H linewidths and distorted signal intensities. The former observation can be attributed to minor experimental imperfections which allow unwanted ^{1}H magnetization to sneak through, while the latter effects appear to arise from different relaxation properties of the IS-spin states for the two detection methods. With respect to the linewidths, it should be noted that in the ^{15}N-detecting HSQC experiment the ^{1}H resonances are observed during t_1 through the correlated state $\mathbf{I}_{X,Y}\mathbf{S}_Z$, which appears to be a little more sensitive to line broadening effects than ^{1}H transverse magnetization, such that the ^{1}H resonance lines are slightly narrower when ^{1}H detection is used. Concerning the distortion of signal intensities, it should be taken into consideration that during the second recoupling period, according to the experimental schemes shown in Figs. 1a and 1b, the detected spin, respectively, is selected via a state of transverse magnetization. Hence, in the ^{1}H-detecting REPT-HSQC experiment, the heteronuclear correlations are more strongly subject to homonuclear ^{1}H couplings. The resulting relaxation effect can lead to distortions of the signal intensities of the strong correlations and, moreover, explains the absence of weak signals indicating longer distance NH correlations. To overcome this relaxation problem, the inversely detected experiment could be designed such that the IS-states pass through a transverse S-state instead of a transverse I-state during the second recoupling period, but then the suppression of unwanted ^{1}H magnetization was found to be much less efficient.

Unquestionably, the major goal of employing inverse detection on ^{1}H is the improvement of the signal quality. To demonstrate the effect of inverse detection on the experimental signal-to-noise ratio (S/N), Fig. 5 shows ^{15}N slices taken from the two-dimensional REPT-HSQC spectra in Fig. 4 at the H^a (13.2 ppm) and H^b (11.0 ppm) resonance for the keto and enol compounds, respectively. The signal improvement achievable by ^{1}H detection is obvious, with the S/N being enhanced by factors of 6 and 10, respectively. This enhancement effect has already been discussed in detail by Ishii and Tycko (*30*) for solid-state ^{15}N spectra obtained under fast MAS conditions, although the comparison of a straight ^{1}H–^{15}N CPMAS with a double-CP experiment yielded slightly smaller enhancement factors between 2 to 3.2. This lower sensitivity gain is probably caused by the additional second CP step which is required for the inverse detection scheme used in Ref. (*30*), while the REPT-HSQC approach presented here is almost perfectly symmetrical with respect to ^{15}N- and ^{1}H-detection. However, as a side effect, it should again be noted that the signals of the weaker NH

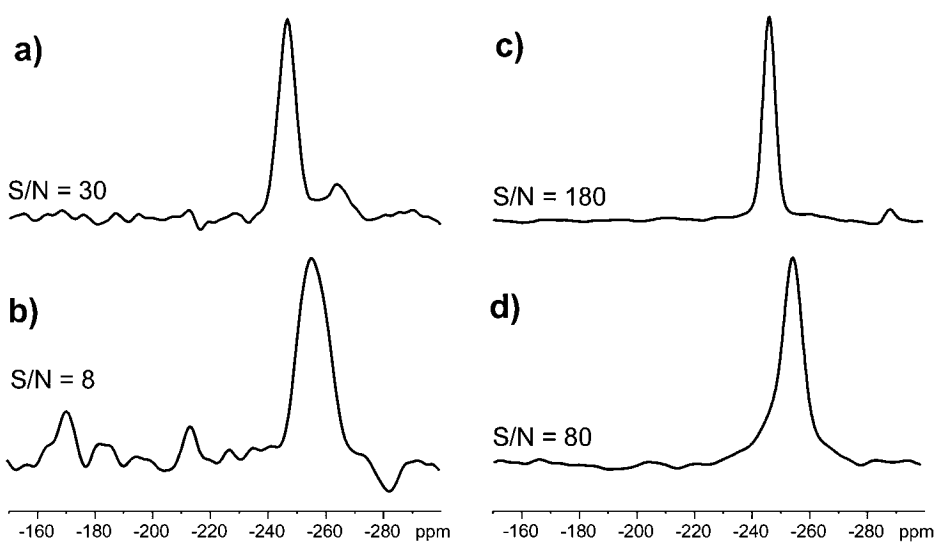

FIG. 5. ^{15}N-Slices from the two-dimensional ^{1}H–^{15}N REPT-HSQC spectra shown in Fig. 4. For the keto (a and c) and the enol (b and d) compounds, the slices are taken at the H^a (13.2 ppm) and H^b (11.0 ppm) resonances, respectively. The spectra allow the comparison of the signal-to-noise ratios (S/N) obtained by ^{15}N-detection (a and b) and ^{1}H-detection (c and d). The enol spectra exhibit a lower S/N, because the spin–lattice relaxation time is significantly longer for the enol- than for the keto-dimers.

correlations due to N···H hydrogen bonds appear to benefit less from ^{1}H detection. However, by applying longer recoupling times the weaker correlations are clearly observed (not shown).

4.3. ^{1}H–^{15}N REPT-HSQC Filtered ^{1}H–^{1}H DQ Spectra

The inverse REPT-HSQC approach can not only be used as an alternative detection method for heteronuclear correlation spectra, as shown above, but also as a filter selecting ^{1}H signals for subsequent ^{1}H experiments, according to Eq. [13]. In Fig. 6, the performance of the ^{1}H signal selection by ^{1}H–^{15}N REPT-HSQC is demonstrated for the keto and enol compound. The ^{1}H MAS spectra are recorded using the pulse sequence depicted in Fig. 1b with $t_1 = 0$. Applying a short recoupling period of two rotor periods, the signals of the protons with the shortest distances to nitrogen atoms, i.e., the protons chemically bonded to nitrogens, are selected: H^a and H^b for the keto and only H^b for the enol compound (see structures in Fig. 2). Conversely, the aliphatic ^{1}H signal is reduced to <3% of its intensity in a ^{1}H MAS one-pulse experiment and is observed with ill-defined phase. Due to the statistics of the ^{15}N enrichment, H^a and/or H^b are bonded to ^{15}N in only one of *three* molecules, such that unwanted ^{1}H signal is effectively reduced to <1% of its original intensity.

Such a REPT-HSQC filter can, for example, be combined with a ^{1}H–^{1}H DQ experiment. Under fast MAS, ^{1}H–^{1}H DQ experiments have been proved to provide important and detailed information about proton–proton proximities, which have been particularly useful for the investigation of hydrogen-bonded structures (*5*, *50*). In some cases, however, an additional ^{1}H signal selection procedure may be helpful in order to remove unwanted intense peaks and/or to unravel superimposed peaks in the two-dimensional DQ spectrum. In fact, the ^{1}H–^{1}H DQ spectra of the hydrogen-bonded dimers investigated here are sufficiently resolved under fast MAS conditions and allow an unambiguous assignment of all ^{1}H resonances except for the distinction of methylene and methyl positions in the alkyl chains. Hence, these spectra are well suited to demonstrating the features of ^{15}N-edited ^{1}H–^{1}H DQ spectroscopy.

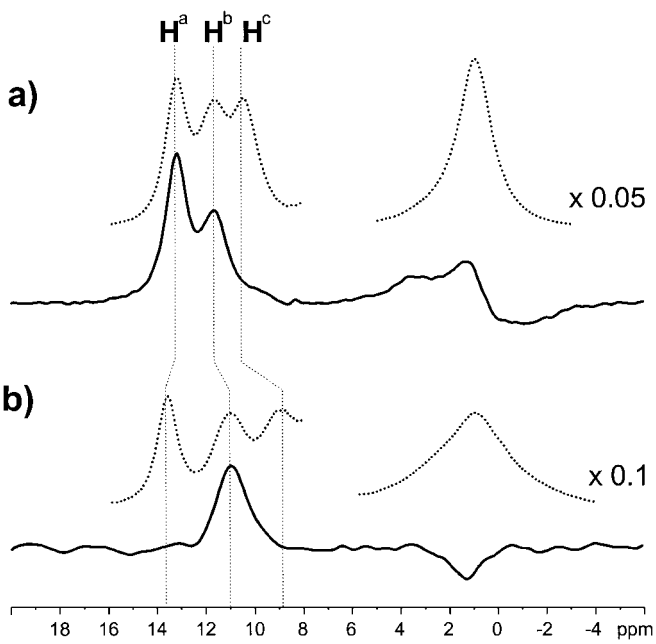

FIG. 6. ^{1}H–^{15}N REPT-HSQC filtered ^{1}H MAS spectra of the keto (a) and the enol dimers (b). The selection efficiency of the heteronuclear filter is demonstrated by the comparison with the regular ^{1}H MAS spectra of the two compounds (dotted lines).

First consider the ^{1}H–^{1}H DQ spectra obtained for the keto and enol compound without any further ^{1}H signal selection (Figs. 7a and 8a, respectively). Both DQ spectra are dominated by intense aliphatic signals which are irrelevant and rather disturbing for the investigation of the arrays of hydrogen bonds. With respect to the latter, the DQ signals involving only the amide protons (H^a, H^b, H^c) are the most interesting part of the spectrum. In Fig. 7a, the strong H^b–H^b and H^b–H^c DQ signals provide evidence for close H^b–H^b and H^b–H^c proximities, which are consistent with the quadruple hydrogen bond formed by the keto compound (see Fig. 2) and, conversely, enable the unique assignment of these two resonances. Considering the signals of DQCs between amide and aliphatic protons, strong H^a–H^{aliph} and H^c–H^{aliph} coherences, but only a very weak H^b–H^{aliph} coherence are observed, because H^a and H^c are close to the $C_{13}H_{27}$ and C_4H_9 chains, respectively, whereas the two H^b in the center of the quadruple hydrogen bond are further away from the alkyl protons. A noteworthy feature is the appearance of a H^d–H^d peak indicating an *inter*molecular rather than an *intra*molecular proximity between two vinyl protons H^d, since the H^d–H^d distance within a single hydrogen-bonded dimer is far too large. Thus, this peak is highly valuable as an indication of the packing of the molecules in the keto form.

The ^{1}H–^{1}H DQ spectrum of the enol compound (Fig. 8a) shows intense H^b–H^b and H^a–H^b DQCs, but no evidence for a H^b–H^c DQ signal. This indicates that in the enol-dimers H^b is no longer close to H^c, but to H^a, while the H^b–H^b proximity remains unchanged. Considering the DQ peaks between the amide and aliphatic protons, the H^b–H^{aliph} signal is still the weakest. These features of the ^{1}H–^{1}H DQ spectrum agree with the quadruple hydrogen bond formed by the enol tautomer and again allow the resonances to be unambiguously assigned. In comparison to Fig. 7a, a clear distinction of the two dimers is easily possible. Moreover, a different packing behavior of the two compounds can be concluded from the presence and the absence of the H^d–H^d DQ peak in Figs. 7a and 8a, respectively. It should be pointed out that for amide-aliphatic DQCs no corresponding DQ peaks are observed at the aliphatic ^{1}H resonance in either spectrum. These signals are obscured by the presence of t_1-noise and baseline distortions (the negative intensity, due to which, is not shown in the spectra) associated with the intense signal of purely aliphatic DQCs. The t_1-noise arises as a consequence of the mobility of the $C_{13}H_{27}$ chains.

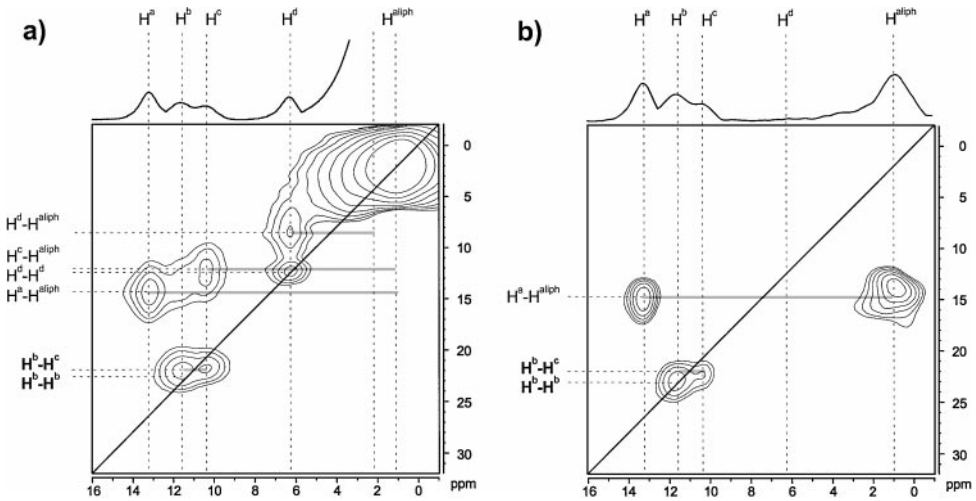

FIG. 7. Two-dimensional ^{1}H–^{1}H DQ spectrum of the keto dimer, recorded under MAS at 30 kHz applying homonuclear ^{1}H–^{1}H dipolar recoupling for a duration of one rotor period for the excitation and reconversion of ^{1}H–^{1}H DQCs: (a) Regular ^{1}H–^{1}H DQ experiment. (b) ^{1}H–^{1}H DQ experiment carried out on ^{1}H magnetization which has passed a preceding ^{1}H–^{15}N REPT-HSQC filter selecting the H^a and H^b resonances by means of ^{1}H–^{15}N dipolar couplings. Consequently, only strong DQCs involving H^a or H^b can be observed, while the other DQ signals are removed.

By applying a ^{1}H–^{15}N REPT-HSQC filter with short recoupling periods prior to the ^{1}H–^{1}H DQ experiment, the initial ^{1}H magnetization available for the generation of DQCs is restricted to those protons which are chemically bonded to ^{15}N, i.e., H^a and H^b for the keto compound and only H^b for the enol compound. Consequently, only ^{1}H–^{1}H DQCs can be observed, in which one of the selected protons is involved, while all other DQCs, such as the purely aliphatic ones, are suppressed. The simplifying effect on the resulting DQ spectra for the keto and enol dimers is clearly demonstrated by comparing Figs. 7a and 8a with Figs. 7b and 8b, respectively.

For the keto compound, the REPT-HSQC filter reduces the observed DQ signals to only the H^b–H^b and H^b–H^c DQ signal pattern as well as to the pair of H^a–H^{aliph} DQ peaks (Fig. 7b). Note that the H^a–H^{aliph} DQ signal at the aliphatic resonance can be recovered by the removal of the intense aliphatic DQ signal, although the phase of the peak is still slightly distorted by weak t_1-noise, which is now due to traces of ^{1}H magnetization passing through the REPT-HSQC filter. In contrast to H^a–H^{aliph}, no H^b–H^{aliph} DQ signals are observed, indicating that the H^b–H^{aliph} dipolar couplings are too weak. The weakness of this coupling agrees with the structure of the dimer (Fig. 2) and is also reflected

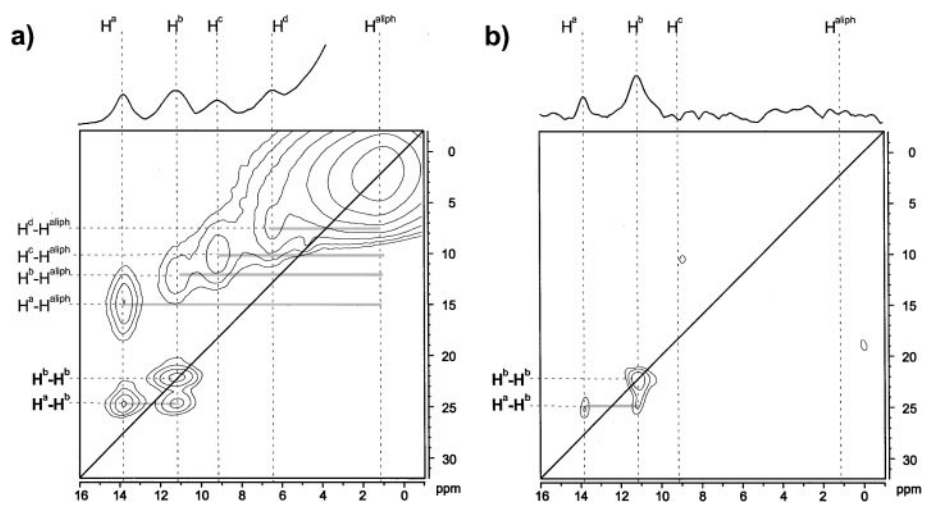

FIG. 8. Two-dimensional ^{1}H–^{1}H DQ spectrum of the enol dimer, recorded under MAS at 30 kHz applying homonuclear ^{1}H–^{1}H dipolar recoupling for a duration of one rotor period for the excitation and reconversion of ^{1}H–^{1}H DQCs: (a) Regular ^{1}H–^{1}H DQ experiment. (b) ^{1}H–^{1}H DQ experiment carried out on ^{1}H magnetization which has passed a preceding ^{1}H–^{15}N REPT-HSQC filter selecting the H^b resonance by means of ^{1}H–^{15}N dipolar couplings. Consequently, only strong DQCs involving H^b can be observed, while the other DQ signals are removed.

in the unfiltered ^{1}H–^{1}H DQ spectrum (Fig. 7a), where the H^b–H^{aliph} DQ signals are the weakest of the amide-aliphatic DQCs. Note that the appearance of a H^b–H^{aliph} peak in Fig. 7a could be aided by the presence of shoulders of the stronger H^a–H^{aliph} and H^c–H^{aliph} DQ peaks nearby. By applying the REPT- HSQC filter to the enol compound, the ^{1}H–^{1}H DQ signals are reduced to the H^b–H^b and H^a–H^b DQ signals, because here the DQ experiment starts with H^b magnetization only and H^b is not involved in any further strong DQCs. Again, the H^b–H^{aliph} dipolar coupling does apparently not suffice to produce a DQ signal in the filtered DQ spectrum.

In general, a ^{1}H–^{1}H DQ signal intensity depends on the product of the ^{1}H–^{1}H dipolar coupling strength and the experimental recoupling time used for the generation of the DQCs (*4*). However, in the filtered versions of the DQ experiments, the signal intensities additionally rely on the ^{1}H–^{15}N dipolar couplings and the heteronuclear recoupling periods during the REPT-HSQC selection procedure, resulting in an approximate overall dependence according to Eq. [16] for short recoupling times. For the samples used here, a statistical factor needs to be taken into account in addition to the weighting factor $\Omega_D^{IS}(0, N\tau_R)$, because the isocytosine nitrogens are, on average, only 33% ^{15}N-enriched. Thus, the combined effects of signal filtration and isotopic enrichment scheme lead to a significant reduction of the DQ signal intensity in the REPT-HSQC filtered experiments, compared to the unfiltered ^{1}H–^{1}H DQ spectra. In particular, only H^b can form H^b–H^b DQCs involving *two* protons selected via ^{1}H–^{15}N REPT-HSQC, but even two-thirds of the H^b–H^b DQCs contain only *one* selected H^b. All other DQCs observed in the filtered spectra (i.e., H^b–H^c and H^a–H^{aliph} for the keto and H^a–H^b for the enol dimer) involve only *one* selected proton. For a quantitative interpretation of the signal intensities, all of these factors need to be taken into account, plus the effects of relaxation during the pulse sequence due to residual homonuclear ^{1}H–^{1}H dipolar couplings, etc. However, the signals observed in REPT-HSQC filtered ^{1}H–^{1}H DQ spectra can be straightforwardly understood on a semi-quantitative basis, which thoroughly suffices to demonstrate the capability of the experiment with respect to ^{1}H signal selection.

5. CONCLUSIONS AND OUTLOOK

The feasibility of inverse, i.e., ^{1}H, detection for ^{1}H–^{15}N heteronuclear MAS correlation experiments in the solid state has been demonstrated using hydrogen-bonded dimers of ^{15}N-labeled 2-ureido-4[^{1}H]-pyrimidinone moieties as an example. Under fast MAS, the HSQC experiment applied here (*12*) makes use of recoupled polarization transfer which, in contrast to CP techniques, allows a symmetrical design for conventional and inverse detection schemes. As a major advantage of inverse detection, signal enhancement factors between 5 and 10 were experimentally observed in ^{1}H–^{15}N REPT-HSQC spectra. In the inverse-detection experiments, efficient suppression of unwanted ^{1}H magnetization to a degree of <1% could be achieved by RF pulses and phase cycling schemes, but without the help of PFGs.

This efficiency permits the REPT-HSQC technique to be readily used as a filter selecting the signals of protons which are (or, alternatively, are not) dipolar-coupled to ^{15}N or another heteronucleus. As an example, we have coupled such a ^{1}H–^{15}N REPT-HSQC filter to a ^{1}H–^{1}H DQ experiment such that the initial ^{1}H magnetization available for the generation of ^{1}H–^{1}H DQCs is restricted to protons which are strongly coupled to ^{15}N. In this way, DQ signals can be selectively observed and perturbing ones removed from the two-dimensional spectra. In a sense, this REPT-HSQC filtration procedure is the inverse version of a ^{1}H experiment, whose signal is transferred to a heteronucleus for detection, for example, by means of a conventional cross-polarization step following a ^{1}H double- or multiple-quantum experiment (*59, 60*). The latter approach may take advantage from the chemical-shift resolution properties of the heteronucleus, but the application of a preceding filter, in return, is able to preserve the significant sensitivity gain inherent to ^{1}H detection under fast MAS. Moreover, an additional heteronuclear (e.g., ^{13}C or ^{15}N) spectral dimension can readily be embedded in the REPT-HSQC filter such that the experiment yields three-dimensional ^{13}C–^{1}H–^{1}H or ^{15}N–^{1}H–^{1}H HSQC/DQ spectra.

The inverse-detection technique presented here can potentially be further improved by optimizing the NMR probes for ^{1}H detection as well as by the application of pulsed field gradients for signal selection and/or suppression. In analogy to well-established liquid-state NMR techniques and with little demands on the homogeneity of the gradient field, the dephasing and rephasing of transverse magnetization would allow the desired coherences to be selected in a single transient of the experiment. Consequently, the sensitivity of the receiver could be adjusted to the amplitude of the incoming signal of interest, and the phase cycling procedure involving the subtraction of relatively intense signals from each other could be avoided. Further work along these lines is in progress.

ACKNOWLEDGMENTS

The authors thank Kay Saalwächter for helpful comments on the implementation of the REPT technique as well as Steven P. Brown for carefully checking the manuscript. B.L. acknowledges financial support from the Deutsche Forschungsgemeinschaft.

REFERENCES

1. M. Mehring, "Principles of High Resolution NMR in Solids," Springer-Verlag, Berlin, 1983.
2. K. Schmidt-Rohr and H. W. Spiess, "Multidimensional Solid-State NMR and Polymers," Academic Press, London, 1994.
3. I. Schnell, A. Lupulescu, S. Hafner, D. E. Demco, and H. W. Spiess, Resolution enhancement in multiple-quantum MAS NMR spectroscopy, *J. Magn. Reson.* **133,** 61–69 (1998).
4. I. Schnell and H. W. Spiess, ^{1}H NMR spectroscopy in the solid state: Very-fast sample spinning and multiple-quantum coherences, *Adv. Opt. Magn. Reson*, in press.

5. I. Schnell, S. P. Brown, H. Y. Low, H. Ishida, and H. W. Spiess, An investigation of hydrogen bonding in benzoxazine dimers by fast magic-angle spinning and double-quantum ^{1}H NMR spectroscopy, *J. Am. Chem. Soc.* **120,** 11784–11795 (1998).
6. C. Filip, S. Hafner, I. Schnell, D. E. Demco, and H. W. Spiess, Solid-state nuclear magnetic resonance spectra of dipolar-coupled multi-spin systems under fast magic angle spinning, *J. Chem. Phys.* **110,** 423– 440 (1999).
7. D. F. Shantz, J. Schmedt a. d. Günne, H. Koller, and R. F. Lobo, Multiple-quantum ^{1}H MAS NMR studies of defect sites in as-made all-silica ZSM-12 zeolite, *J. Am. Chem. Soc.* **122,** 6659–6663 (2000).
8. S. P. Brown, I. Schnell, J. D. Brand, K. Müllen, and H. W. Spiess, An investigation of π–π packing in a columnar hexabenzocoronene by fast magic-angle spinning and double-quantum ^{1}H solid-state NMR spectroscopy, *J. Am. Chem. Soc.* **121,** 6712–6718 (1999).
9. B.-J. van Rossum, H. Förster, and H. J. M. de Groot, High-field and high-speed CPMAS ^{13}C NMR heteronuclear dipolar-correlation spectroscopy of solids with frequency-switched Lee–Goldburg homonuclear decoupling, *J. Magn. Reson.* **124,** 516–519 (1997).
10. A. Lesage, D. Sakellariou, S. Steuernagel, and L. Emsley, Carbon-proton chemical shift correlation in solid-state NMR by through bond multiple-quantum spectroscopy, *J. Am. Chem. Soc.* **120,** 13194–13201 (1998).
11. K. Saalwächter, R. Graf, and H. W. Spiess, Recoupled polarization transfer heteronuclear ^{1}H–^{13}C multiple-quantum correlation in solids under ultra-fast MAS, *J. Magn. Reson.* **140,** 471–476 (1999).
12. K. Saalwächter, R. Graf, and H. W. Spiess, Recoupled polarization-transfer methods for solid-state ^{1}H–^{13}C heteronuclear correlation in the limit of fast MAS, *J. Magn. Reson.* **148,** 398- 418 (2001).
13. K. Saalwächter and H. W. Spiess, Heteronuclear ^{1}H–^{13}C multiple-spin correlation in solid-state NMR: Combining REDOR recoupling and multiple-quantum spectroscopy, *J. Chem. Phys.* **114,** 5707–5728 (2001).
14. M. Baldus, Solid-state NMR in immobilized biomolecules: Correlation experiments for assignment and structure determination in fully labeled peptides and membrane-proteins, *in* Proceedings of the International Workshop "The Future of Solid State NMR in Biology," Leiden, The Netherlands, 2000.
15. A. Bielecki, A. C. Kolbert, and M. H. Levitt, Frequency-switched pulse sequences—Homonuclear decoupling and dilute spin NMR in solids, *Chem. Phys. Lett.* **155,** 341–346 (1989).
16. M. H. Levitt, A. C. Kolbert, A. Bielecki, and D. J. Ruben, High-resolution ^{1}H NMR in solids with frequency-switched pulse sequences, *Solid State NMR* **2,** 151–163 (1993).
17. A. A. Maudsley, L. Müller, and R. R. Ernst, Cross-correlation of spin-decoupled NMR spectra by heteronuclear two-dimensional spectroscopy, *J. Magn. Reson.* **28,** 463– 469 (1977).
18. L. Müller, Sensitivity enhanced detection of weak nuclei using heteronuclear multiple quantum coherence, *J. Am. Chem. Soc.* **101,** 4481– 4484 (1979).
19. A. Bax, R. H. Griffey, and B. L. Hawkins, Correlation of proton and nitrogen-15 chemical shifts by multiple quantum NMR, *J. Magn. Reson.* **55,** 301–315 (1983).
20. G. Bodenhausen and D. J. Ruben, Natural abundance nitrogen-15 NMR by enhanced heteronuclear spectroscopy, *Chem. Phys. Lett.* **69,** 185–189 (1980).
21. A. G. Redfield, Stimulated echo NMR spectra and their use for heteronuclear two-dimensional shift correlation, *Chem. Phys. Lett.* **96,** 537 (1983).
22. R. R. Ernst, G. Bodenhausen, and A. Wokaun, "Principles of Nuclear Magnetic Resonance in One and Two Dimensions," Oxford Univ. Press, Oxford, 1987.
23. G. Otting and K. Wüthrich, Efficient purging scheme for proton-detected heteronuclear two-dimensional NMR, *J. Magn. Reson.* **76,** 569–574 (1988).
24. S. R. Hartmann and E. L. Hahn, Nuclear double resonance in the rotating frame, *Phys. Rev.* **128,** 2042–2053 (1962).
25. F. M. Lurie and C. P. Slichter, Spin temperature in nuclear double resonance, *Phys. Rev. A* **133,** 1108–1122 (1964).
26. H. E. Bleich and A. G. Redfield, Higher resolution NMR of rare spins in solids, *J. Chem. Phys.* **55,** 5405–5406 (1971).
27. C. S. Yannoni, High-resolution NMR in solids by intermolecular double resonance, *J. Chem. Phys.* **56,** 1773–1774 (1972).
28. P. K. Grannell, P. Mansfield, and M. A. B. Whitaker, ^{13}C double-resonance Fourier-transform spectroscopy in solids, *Phys. Rev. B* **8,** 4149–4163 (1973).
29. A. Pines, M. G. Gibby, and J. S. Waugh, Proton-enhanced NMR of dilute spins in solids, *J. Chem. Phys.* **59,** 569–590 (1973).
30. Y. Ishii and R. Tycko, Sensitivity enhancement in solid state ^{15}N NMR by indirect detection with high-speed magic angle spinning, *J. Magn. Reson.* **142,** 199–204 (2000).
31. A. A. Maudsley, A. Wokaun, and R. R. Ernst, Coherence transfer echoes, *Chem. Phys. Lett.* **55,** 9–14 (1978).
32. A. Bax, P. G. de Jong, A. F. Mehlkopf, and J. Smidt, Separation of the different orders of NMR multiple-quantum transitions by the use of pulsed-field gradients, *Chem. Phys. Lett.* **69,** 567–570 (1980).
33. P. Barker and R. Freeman, Pulsed field gradients in NMR. An alternative to phase cycling, *J. Magn. Reson.* **64,** 334–338 (1985).
34. A. Bax and S. S. Pochaapsky, Optimized recording of heteronuclear NMR spectra using pulsed-field gradients, *J. Magn. Reson.* **99,** 638–643 (1992).
35. M. Sattler, J. Schleucher, and C. Griesinger, Heteronuclear multidimensional NMR experiments for the structure determination of proteins in solution employing pulsed field gradients, *Progr. NMR Spectrosc.* **34,** 93–158 (1999).
36. T. Gullion and J. Schaefer, Detection of weak heteronuclear dipolar couplings by rotational-echo double-resonance nuclear magnetic resonance, *Adv. Magn. Reson.* **13,** 57–83 (1989).
37. A. W. Hing, S. Vega, and J. Schaefer, Transferred-echo double-resonance NMR, *J. Magn. Reson.* **96,** 205–209 (1992).
38. A. W. Hing, S. Vega, and J. Schaefer, Measurement of heteronuclear dipolar coupling by transferred-echo double-resonance NMR, *J. Magn. Reson. A* **103,** 151–162 (1993).
39. H. Geen, J. J. Titman, J. Gottwald, and H. W. Spiess, Solid-state proton multiple-quantum NMR spectroscopy with fast magic-angle spinning, *Chem. Phys. Lett.* **227,** 79–86 (1994).
40. J. Gottwald, D. E. Demco, R. Graf, and H. W. Spiess, High-resolution double-quantum NMR spectroscopy of homonuclear spin pairs and proton connectivities in solids, *Chem. Phys. Lett.* **243,** 314–323 (1995).
41. A. E. Bennett, R. G. Griffin, and S. Vega, Recoupling of homo- and heteronuclear dipolar interaction in rotating solids, *in* "NMR Basic Principles and Progress" (P. Diehl, E. Fluck, H. Günter, R. Kosfeld, and J. Seelig, Eds.), Vol. 33, pp. 1–77. Springer-Verlag, Berlin, 1994.
42. D. Marion and K. Wüthrich, Application of phase-sensitive two-dimensional correlated spectroscopy (COSY) for measurements of ^{1}H–^{1}H spin–spin coupling constants in proteins, *Biochem. Biophys. Res. Commun.* **113,** 967–974 (1983).
43. U. Friedrich, I. Schnell, S. P. Brown, A. Lupulescu, D. E. Demco, and H. W. Spiess, Spinning sideband patterns in multiple-quantum magic-angle spinning NMR spectroscopy, *Mol. Phys.* **95,** 1209–1227 (1998).
44. R. Graf, D. E. Demco, J. Gottwald, S. Hafner, and H. W. Spiess, Dipolar couplings and internuclear distances by double-quantum nuclear magnetic resonance spectroscopy of solids, *J. Chem. Phys.* **106,** 885–895 (1997).
45. A. Fechtenkötter, K. Saalwächter, M. A. Harbison, K. Müllen, and H. W. Spiess, Highly ordered columnar structures from hexa-*peri*-hexabenzocoronenes—Synthesis, X-ray diffraction, and solid-state

hetero nuclear multiple-quantum NMR investigations. *Angew. Chem. Int. Ed. Engl.* **38,** 3039–3042 (1999).

46. C. A. Fyfe, J. Skibsted, H. Grondey, and H. M. zu Altenschildesche, Pulsed field gradient multiple-quantum MAS NMR spectroscopy of half-integer spin quadrupolar nuclei, *Chem. Phys. Lett.* **281,** 44–48 (1997).

47. W. E. Maas, A. Bielecki, M. Ziliox, F. H. Laukien, and D. G. Cory, Magnetic field gradients in solid state magic angle spinning NMR, *J. Magn. Reson.* **141,** 29–33 (1999).

48. T. Fritzhanns, S. Hafner, D. E. Demco, H. W. Spiess, and F. H. Laukien, Pulsed field gradient selection in two-dimensional magic angle spinnig NMR spectroscopy of dipolar solids, *J. Magn. Reson.* **134,** 355–359 (1998).

49. S. P. Brown, I. Schnell, J. D. Brand, K. Müllen, and H. W. Spiess, A ^{1}H double-quantum magic-angle spinning solid-state NMR investigation of packing and dynamics in triphenylene and hexabenzocoronene derivatives, *J. Mol. Struct.* **521,** 179–195 (2000).

50. S. P. Brown, I. Schnell, J. D. Brand, K. Müllen, and H. W. Spiess, The competing effects of π–π packing and hydrogen bonding in a hexabenzocoronene carboxylic acid derivative: A ^{1}H solid-state MAS NMR investigation, *Phys. Chem. Chem. Phys.* **2,** 1735–1745 (2000).

51. J.-M. Lehn, "Supramolecular Chemistry," VCH, New York, 1995.

52. F. H. Beijer, Ph.D. thesis, Eindhoven University of Technology, The Netherlands, 1998.

53. R. P. Sijbesma, F. H. Beijer, L. Brunsveld, B. J. B. Folmer, J. H. K. K. Hirschberg, R. F. M. Lange, J. K. L. Lowe, and E. W. Meijer, Reversible polymers fromed from self-complementary monomers using quadruple hydrogen bonding, *Science* **278,** 1601–1604 (1997).

54. F. H. Beijer, R. P. Sijbesma, H. Kooijman, A. L. Spek, and E. W. Meijer, Strong dimerization of ureidopyrimidones via quadruple hydrogen bonding, *J. Am. Chem. Soc.* **120,** 6761–6769 (1998).

55. S. H. M. Söntjens, R. P. Sijbesma, M. H. P. van Genderen, and E. W. Meijer, Stability and lifetime of quadruply hydrogen-bonded 2-ureido-4[^{1}H]-pyrimidinone dimers, *J. Am. Chem. Soc.* **122,** 7487–7493 (2000).

56. A. E. Bennett, C. M. Rienstra, M. Auger, K. V. Lakshmi, and R. G. Griffin, Heteronulcear decoupling in rotating solids, *J. Chem. Phys.* **103,** 6951– 6958 (1995).

57. M. Feike, D. E. Demco, R. Graf, J. Gottwald, S. Hafner, and H. W. Spiess, Broadband multiple-quantum NMR spectroscopy, *J. Magn. Reson. A* **122,** 214–221 (1996).

58. Here, all ^{15}N chemical shift values are given relative to $CH_3{}^{15}NO_2$ (0 ppm) using the two resonances of $^{15}NH_4{}^{15}NO_3$ (-358 and -5 ppm) as a secondary reference. In the literature, ^{15}N chemical shift scales may also be referenced with respect to $^{15}NH_3$, whose resonance is at -380 ppm on the $CH_3{}^{15}NO_2$ scale.

59. Y. Ba and S. Veeman, Multiple-quantum nuclear magnetic resonance spectroscopy of coupled spin 1/2 in solids: Combination with cross polarization and magic-angle spinning, *Solid State NMR* **3,** 249 (1994).

60. B. Reif, C. P. Jaroniec, C. M. Rienstra, and R. G. Griffin, ^{1}H-related MAS correlations in deuterated peptides, 22nd Discussion Meeting, Gesellschaft Deutscher Chemiker—Fachgruppe Magnetische Resonanzspektroskopie, Regensburg, Germany, 2000.